DYNAMIC HARDNESS DURING DIFFERENT PHASES OF INDENTATION

Vytautas Vasauskas
Kaunas University of Technology, Lithuania.

Abstract. The paper reports on the underlying concept for securing the measuring basis used in the method of dynamic hardness which employes one of the standard indentation methods and various shapes of indenter. The complete dynamic indentation cycle can be divided into the three following phases: starting phase, indentation phase and rebound phase. The value for several engineering metals obtained dynamic hardness in various phases of indentation was 1.12 – 1.40 higher than the static hardness.

1. Introduction

There is a fundamental difference between static and dynamic hardness testing: in static tests the effective force acting on the penetration indenter is clearly and comprehensively determined throughout the entire process of indentation into the specimen [1]. In the case of dynamic indentation, however, the load (*F*) acting on the indenter changes during the various phases of the impact cycle [2, 3]. The depth of penetration together with the known geometry of the indenter provides an indirect measure of the area (volume) of contact at full load, from which the mean contact pressure, and thus hardness, may be estimated [4]. The present work reviews these two most commonly used methods of analysis of dynamic indentation test data and their associated corrections. A measurement for determining the dynamic hardness that parallels the method for static hardness determination pertinent to moderate velocity impact was obtained.

2. Background

Conventional dynamic hardness test methods are based almost exclusively on the measurement of the potential residual energy [1]. It is disadvantage for all test methods developed in recent years that for practical application, reference to the standardized procedures is always required. In very many cases the difference between a calibration machine and a series-procedures hardness tester seems not to be entirely understood [3].

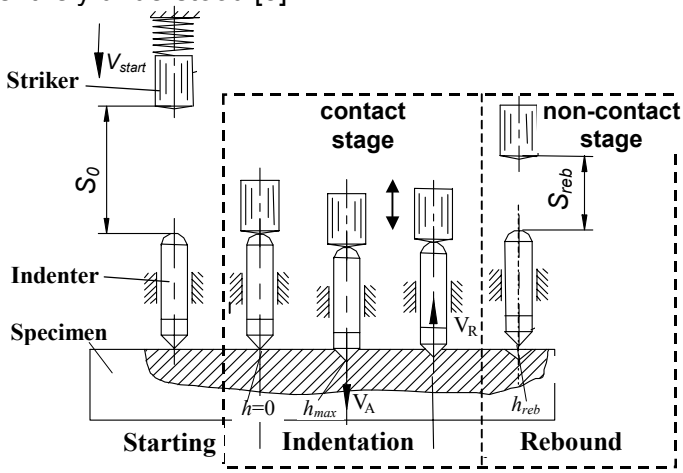

Fig. 1. Dynamic hardness indentation test phases for triple striker – indenter – specimen system: starting, indentation and rebound phases. Contact or non – contact stages for indenter specimen system are evident

The dynamic hardness value during impact is equal to the energy expended in producing the indentation after rebound has occurred (=energy of impact minus energy of rebound) divided by the volume of indentation [1]. A different approach was adopted in testers called Shore rebound

scleroscopes, where the height of the rebound itself is used as a measure of the dynamic scleroscope hardness. If the height of the fall is constant, the height of the rebound is roughly proportional to the static hardness of the material concerned. The second is the energy quotient return (EQUOTIP) method where the energy loss in the elastic-plastic contact is evaluated electronically from the ratio of the velocities of the indenter before and after impact [3]. During the process, the impact velocity V_A and the rebound velocity V_R of the indenter are measured when it is about 1 mm from the test surface. These two measurements are used to determine the EQUOTIP hardness value L by means of the equation L=1000 V_R/V_A.

To allow comparison between the kinetic energies at impact in various types of test the concept of the "equivalent impact energy" was introduced [4]. The complete test procedure for dynamic hardness measurement may be divided into the following stages: starting (striking) phase; indentation phase and rebound phase (Fig. 1). During the starting (striking) phase the potential energy of the testing work-piece is converted into kinetic energy either by free fall or by spring mechanism. Thus for a given contact geometry the intrinsic coefficient of restitution is uniquely determined by the degree of recovery and useful measure of the degree of reversibility of contact deformation. At the end of the indentation process, where the plastic flow of the metal has come to the end and a regime of purely elastic stresses has been reached, the pressure involved in the formation of indentation of the same size under static conditions. Therefore, possible classification of the dynamic hardness measurements must reviewed only for two questions, which deals with the dynamic hardness measurements – contact or non-contact? This method is based on an analysis of the energy that for the residual energy remaining in the impact indenter of a spring activated device and present prior to impact $\frac{cs^2}{2} + mgs + W_f = \frac{mv_k^2}{2}$, where $cs^2/2$ - potential energy of the spring system; mgs – potential gravitational energy; W_f – the energy consumed due to frictional effects along the path s, m-mass of impacting indenter, v_k-incident velocity.

In agreement with the introductory statements above the efficiency of the indentation process is defined as $\eta = W_1 / W_0$, where $W_1 = \int Fdh$ is the work performed on the sample as a result of a single representative impact, and W_0 is the total kinetic energy of the striker. The impact process can be modelled most easily if we assume that a contact dynamic yield pressure p_d (i.e. dynamic hardness, H_d) opposes the indenter. In reality p_d changes continuously during the impact process (Fig. 2). It is converient, initially, to consider the indentation between the indenter and specimen as having two phases, of which the second may be further divided into two stages. Thus the assumed constant p_d will correspond to some "mean" value. In such case, a simple energy balance between the kinetic energy of the impacting indenter and the energy required to form the resulting impression volume gives an expression for dynamic hardness, H_d. For example (Fig. 1), if m is the mass of the impacting indenter, v its incident velocity, v_r is rebound velocity and ΔV the final volume of the impression formed, then $p_d = \frac{0{,}5m(v^2 - v_{reb}^2)}{\Delta V} = H_{dv}$. Invariance of the indentation pressure in hardness measurements requires that the plastic zone volume be governed exclusively by the indentation volume. It follows from this that the indentation volume ΔV be compensated by the misfit induced in the total plastic zone. It has been shown that the relation $\beta = (V_1 / \Delta V)^{1/3} = b/a$ is an important parameter and found the following relation $\frac{H}{\sigma_y} = \frac{2}{3}\left[1 + ln(\beta)^3\right]$, where b is the plastic zone dimension, a is the core radius. Method of energy measurement is based on the measurement of both kinetic energy components, i.e. the impact energy and rebound energy. Deformation model, assume that the volume of impression produced by the impact indenter, is proportional to the kinetic energy, W, of the indenter but is independent of its shape or tip angle, 2θ. Since the volume of a rigid cone with an apex angle of 2θ is $V = \pi / 24 cot\theta\, d^3$, where d is the diameter of the bottom of the right cone $W = VW_o = \pi W_0 / 24 \cdot cot\theta d^3 = W_o k d^3$, where W_o is the

assumedly constant kinetic energy absorbed per unit volume of deformed metal, and $k=\pi \cot \theta / 24$, is a constant.

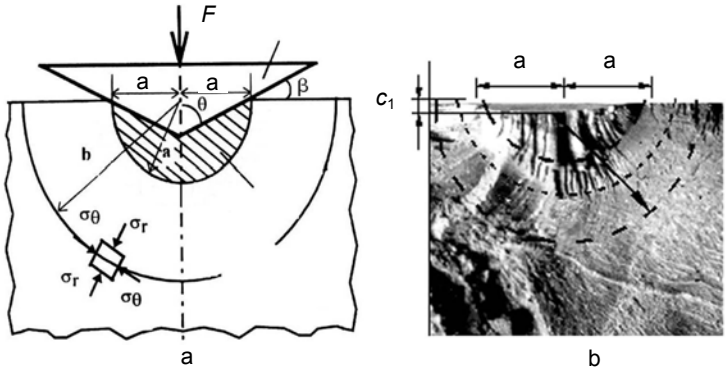

Fig. 2. Indentation volumes for cross-section: a – model for indentation, b – zone of plastic flow in the material underneath the indentation in the test specimen

The load reaches its maximum value at maximum penetration. The load can be derived by taking the hardness $H = \alpha F / h^2$, where α is a constant depending on the geometry of the indenter apex angle and *h* the depth of the surface impression. The maximum penetration during impact can be obtained by equating the fraction of the kinetic energy that is lost during the impact of the indenter on the specimen with the plastic work (W_{pl})

$$W_{pl} = \int_0^{h_{max}} F(z)dz = \frac{1}{2} m v^2 (1 - e^2) \tag{1}$$

where *v* is the impact velocity, h_{max} the maximum penetration, *m* the mass of the indenter, and e the coefficient of restitution. Integration of Eq.(1) leads to an expression for h_{max} which depends on $H^{-1/3}$.

3. Experimental

Dynamic indentation experiments were produced in the specimen by impact in the velocity range 1 to 40 ms^{-1}. As was shown by D.Tabor [1] dynamic effects become significant for impact velocities $\geq$100 ms^{-1}. The conformity of the data to this line indicates that any variation of hardness over the velocity range 5 to 40 ms^{-1} is small. The measurement system consists of an impact device and an electronic indicator device (Fig. 3).

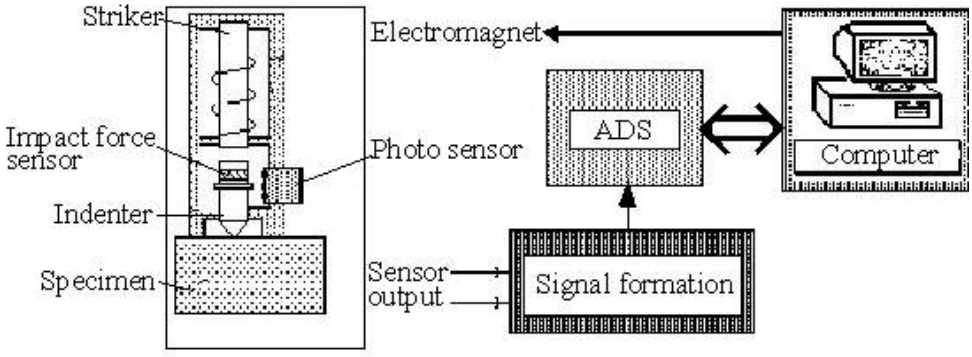

Fig. 3. Schematic of the experimental set-up for dynamic indentation

The impact device fires the impact body against the material to be tested in system striker – indenter – specimen [4]. The detected signals are sampled and processed by the computer, which monitors as well the transducer moves. A piezoelectric transducer sensed loads, while displacements were determined from the indenter travel recorded by means of the photocell. The

piezoelectric transducer (140 kHz resonant) is applied to the indenter, thus ensuring that impact signals can be received even when process is elastic. After further amplification, the signals are analysed for member of counts and intensity (ADS – 10 bits). Function $F(t)$ and $h(t)$ are accounted for 256 – 1024 dots. Choosing striker bars of various lengths can vary the duration of the input pulse and the amplitude of the incident compression stress pulse (or the incident load). Fig.4 shows the indentation depth under load. This represents a condition where the indentor under load is exerting a force that is in equilibrium and apposed by a material- depended force. Evaluations of the dynamic force are summarized in Fig.4, which shows the force at three stages of indentation-rebound stage for metals of various hardness HRC. An examination of the energy balance during the impact indicates that at least 70-80% of the initial kinetic energy of the indenter is dissipated only in plastic deformation in the specimen. The kinetic energy of the rebounding is estimated from measured coefficients of restitution depending on indentation geometry, impact velocity and specimen material. Thus, $W_o = W_1 \cdot \eta_o$, where W_1 is all accumulated initial kinetic energy of striker, η_o is total efficiency for the striker-indenter-specimen set is $\eta_o=\eta_1 \cdot \eta_2$, where η_1=0.9-0.85, η_2 is loss of energy at the indenter-specimen impact for non-linear plastic deformation of cone indenter.

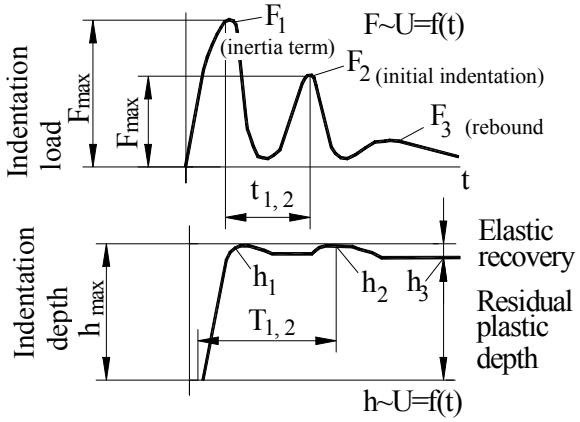

Specimen hardness HRC	F_1, V	$t_{1.2}$, ms	F_2, V	F_3, V
23	0.75243	183	0.32031	0.22313
38	0.82812	139.3	0.49469	0.20875
55	0.61718	101.5	0.60838	0.13281
58	0.69531	98.8	0.61974	0.11719
67	0.70312	86	0.69752	0.04688

Fig. 4. Typical continuous indentation force – displacement curves. Indentation phase corresponds to three waves of deformation

According to Fig. 2 we have $\eta_2 = (1-e_\theta^2)\frac{m_1}{m_1+m_2}$, where e_θ is restitution factor as function of indenter apex angle 2θ, m_1 is striker mass, m_2 is indenter mass; for m_1/m_2=0.5 and cone angles $2\theta=90^o \div 160^o$ η_2=0.5÷0.46. The coefficient of restitution e is, of course not a material property, but a useful measure of the degree of reversibility of the contact deformation processes. $(1-e_\theta^2)$ gives the fraction of the kinetic energy input expended in indentation cycle. It may be seen that the dissipated system energy will be distributed between the striker and indenter in inverse proportion to their relative stiffness. Then total efficiency of the dynamic system in our experiments was for various indentation angles in the ranges 0.336÷0.500.

4. Results and Discussion

The existence of a residual indentation and that the penetration varies with applied contact load F through the indentation cycle (Fig. 4) means that the $F(h)$ curve must show some hysteresis on unloading and indentation volume relaxes elastically. It is apparent from the experimental curves (Fig. 4) that in general the coefficient of restitution of impacting solids capable of undergoing plastic deformation will not be a constant. At the end of the impact where the elastic compression and recovery take place, the plastic flow of the material has come to an end. There is no further bulk displacement of metal around the indenter, and no energy is expended in pushing the metal away from the indentation. All the deformation around the indenter is now of an elastic nature, and any

kinetic energy imported to the material under these conditions should be reversible. As a result the pressure at this stage may be expected to be essentially the same as the mean pressure p_m required to produce plastic yielding and corresponds to the Meyer static hardness number. As the indentation angle decreases, there will be a corresponding decrease in the coefficient of restitution. The constitutive equation describing the mechanical behaviour of elastic-plastic material is generally given by the power-law equation $\sigma=k\cdot\varepsilon^n$, where σ is the flow stress and ε is the true strain. *K* and *n* are the material parameters, where *K* is the strength coefficient, and n is the strain-rate sensitivity factor. We have derived [4] the following equation to describe the plastic deformation of a recovered indentation volume in terms of the indentation diameter (depth): $\varepsilon = \frac{A_1 - A_o}{A_o} = \frac{1}{sin\,\theta} - 1 = ln\,\frac{1}{sin\,\theta}$, where ε - average contact deformation, $A_1 = \pi d^2 / 4 sin\theta$ is surface of indentation, $A_o = \pi d^2 / 4$ – projection area indentation, 2θ is indentation (cone) angle, *d* is diameter of indentation. Estimates of the strain beneath conical indenters, based on simple geometry, indicate values ranging from 0.004 to 0.25 for 170^0 and 90^0 cones respectively.

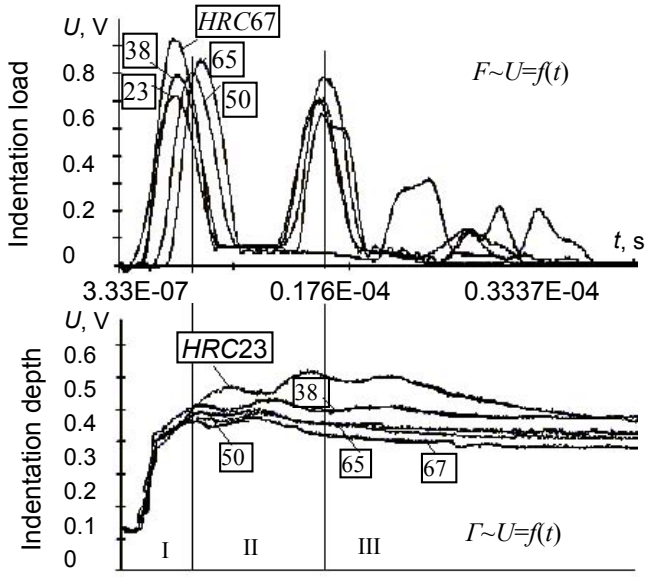

Fig. 5. Typical dynamic indentation force–displacement curves (cone indenter $2\theta = 90^0$) for various steel specimens (hardness *HRC* =23 – 67)

The flow stresses at room temperature change significantly over this range and therefore the hardness depends on cone angle and metals show normal work-hardening properties under these conditions. These characteristics are reflected in the results presented in Fig. 6. Thus all the experiments reported here are based on cone tungsten carbide indenters of angles $60^0<2\theta<180^0$ at the tip. The static hardness is observed to increase as the deformation size increases, indicating that a certain amount of strain hardening has occurred. In dynamic conclusion we have, at first, that when deformation size increases hardness (Fig. 6, a, curve 1) decreases. The dynamic and static hardness measurements obtained from indentation diagrams in contact indentation phase for several metals are shown in Fig. 6, b. The percentage hardness increase in dynamic hardness maximum over the static maximum value, i.e. $(H_d - H_s)/H_s$x100%, is also indicated on the right side of Fig. 6, b. For steels this increase is between 10–20% and for materials like aluminum and copper varies from 1 – 10%. All the deformation around indenter is now of an elastic nature, and any kinetic energy imparted to the material under these conditions should be reversible.

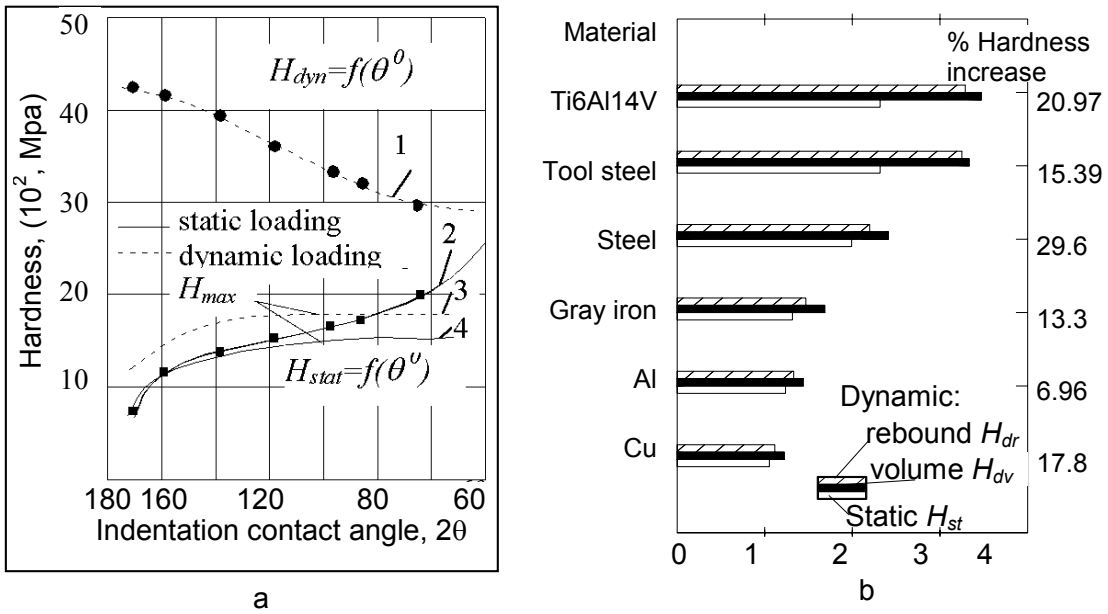

Fig. 6, a - stress-strain curves for static and dynamic indentation hardness: *1, 2*-contact friction unaccounted, *3, 4*-contact friction and efficiency of dynamic system striker-indenter-specimen set accounted; b - summary of static and dynamic indentation hardness measurements for several commercial metals

As a result the pressure at this stage may be expected to be essentially the same as H_{dv}. As shown in fig.5 for the harder metals the value H_{dr} are less than 10% higher than H_{st},.whilst the values H_{dv}.are 20 to 30% higher. With the soft metals the difference between H_{dv}.and H_{dr}.becomes very marked indeed. The dynamic yield pressure H_{dv}.is now very much higher than the static pressure H_{st}.whereas H_{dr}.remains relatively close to the static values. Dynamic hardness is 1,12-1,40 times higher the static hardness, because of the effect of strain rate on the deformation of material. Also we see that value of the friction affects the magnitude of the mean pressures necessary to form the indentations and position of the maximum.

5. Conclusions

The technique parallels the method for static indentation hardness determination and allows direct comparisons between static and dynamic hardness measurements. The dynamic hardness was evaluated from measurements of parameters for various phases of indentation cycle. The dynamic hardness was found 1.12-1.40 higher than hardness determined by static indentation, although the morphology of the damage surrounding the contact site is similar in static loading and impact. It is obviously clear that the above dynamic hardness testing methods does not maintain the simplicity and the low cost of static hardness testing.

6. References

[1] Tabor D. „The Hardness of Metals“, Oxford Univ.Press, London, 1951.
[2] Tirupataiah, Y. and Sundarajan, G. “A Dynamic Indentation Technique for the Characterization of the High Strain Rate Plastic Flow Behaviour of Ductile Metals and Alloys”, J. Mech. Phys. Solids, v.39 (2), 1991, p.p. 243-271.
[3] Leeb, D. “Definition of the Hardness Value “L” in the EQUOTIP Dynamic Measuring Method, in: Hardness testing in theory and practice”, (VDI-Berichte, 583).-Düsseldorf, 1986, p.p. 109-135.
[4] Vasauskas, V. “Geometry effect of indenters on dynamic hardness”,-Proc. of the XVI IMEKO World Congress IMEKO – 2000, v. III.-Austrian Society for Measurement and Automation, Austria, Viena, 2000, p.p. 343-348.